

Reactive adsorption and diffusion of Ti on Si(001) by scanning tunneling microscopy

Kengo Ishiyama* and Yasunori Taga

Toyota Central Research and Development Laboratories Inc., 41-1 Nagakute, Aichi 480-11, Japan

Ayahiko Ichimiya

Department of Applied Physics, Nagoya University, Nagoya 464-01, Japan

(Received 31 August 1994; revised manuscript received 13 October 1994)

Scanning tunneling microscopy has been used to provide the atomic view of the reaction and diffusion of Ti and Si(001) at the monatomic adsorption stage. Two monatomic adsorption structures below and above 440 K have been found. The characteristic adsorption below 440 K is a Ti atom at the pedestal site on a dimer row. The high-temperature adsorption structure above 440 K is adsorption at a dimer vacancy induced by a dimer ejection process on the structural conversion path. The high-temperature adsorption structure shows one-dimensional hopping motion along a dimer row. Measurement of the hop rate gives the activation energy for diffusion and the prefactor of $E_D = 1.8 \pm 0.1$ eV and $\nu_{H0} = 10^{14 \pm 1}$ sec⁻¹, respectively. The growth features and the diffusion mechanism can be interpreted in terms of Ti-Si bond formation.

I. INTRODUCTION

Refractory-metal (RM)/silicon interfaces have attracted increasing interest, since they are of great importance in highly miniaturized semiconductor devices. The strong reactivity of RM's with Si was reported as the interfacial mixing as low as room temperature and the silicide formation at elevated temperature. Such reaction products crucially influence the properties of the RM/Si interfaces, for example, the structural stability at high temperature and high current density, and the Schottky-barrier formation. In many studies on RM/Si systems including the Ti/Si system, electron spectroscopic methods have been used to investigate the chemical behavior and electronic properties at the initial growth of interfaces.¹⁻⁶ For the initial formation of the Ti/Si(111)-2×1 interface at RT, Giudice *et al.*² used core level photoemission spectroscopy to observe the initiation of the Ti-Si reaction as soon as the first Ti reaches the surface, the following growth of TiSi, and then a formation of a solid solution layer up to Ti coverage of 10 Å. Wallart *et al.*³ reported a formation of disordered mixture phase of Ti:Si=5:3-1:1 below 570 K and growth of crystalline TiSi₂ at the higher temperature. They have stressed the importance of mechanisms for the competing processes of diffusion and reaction at RM/Si interfaces which involve, for example, substrate disruption and grain boundary diffusion. However, the close interpretation at the atomic level of those spectroscopic behaviors has been restricted by the limited lateral resolution and the surface sensitivity. Thus the atomic processes at the initiation of the interfacial reaction have not been unveiled yet.

Scanning tunneling microscopy (STM) has a high potential for investigating such surface processes at the atomic level. Noticeably, "hot STM" has demonstrated its particular suitability by the direct imaging of adatom diffusion and reactions at elevated temperature, and has

provided the kinetics of diffusion and reactions on semiconductor surfaces.⁷⁻¹¹

This paper describes the atomic behavior at the initial adsorption stage of evaporated Ti on Si(001) observed by STM. We find two monatomic adsorption structures formed below and above 440 K. In an *in situ* high-temperature observation, we detect a conversion of a Ti atom from the site at the first layer to that at the second layer, which induces ejection of Si dimer atoms. We measured the hopping motion of the adsorption structure formed and obtain the activation energy for diffusion. The observed adsorption reaction and the diffusion mechanism are discussed in terms of Ti-Si bond formation.

II. EXPERIMENT

A Si(001) substrate (Sb doped, 0.01 Ω cm, 7×1×0.3 mm³) was cleaned by HF 1% aqueous solution, H₂SO₄:H₂O₂=4:1 mixture, and finally rinsed in pure H₂O. It was degassed carefully in ultrahigh vacuum (UHV), and finally cleaned by 1200 °C flash-anneal cycles below 1×10⁻¹⁰ Torr. A STM image of the substrate showed a clean 2×1 reconstructed surface with a small number density of dimer vacancies smaller than 1% of the total dimer pairs. Measurements were performed by using a commercial UHV STM (JEOL JSTM-4500VT) equipped with a Ti evaporation source. In the STM, the sample was heated by passing dc current and the temperature was monitored with an infrared pyrometer calibrated with a W-WRe thermocouple. The uncertainty in the measured temperature was estimated at ±10 K. Ti was evaporated from an electron bombarded Ti rod of 2 mm diameter at the rate of 0.0015 ML sec⁻¹, where (ML denotes monolayer), 1 ML= 6.8 × 10¹⁴cm⁻². The

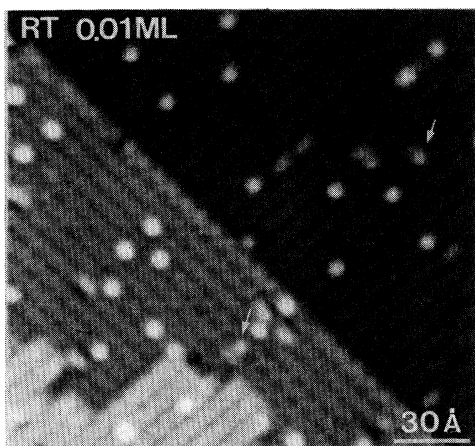


FIG. 1. Morphologies of Si(001)- 2×1 surface with Ti deposited up to $\Theta_{\text{Ti}} = 0.01$ ML. The image is taken at a sample bias of +2 V. Arrows indicate adsorption at valley sites.

deposition rate was measured with a quartz crystal oscillator in the other UHV chamber and the uncertainty of $\pm 10\%$ was estimated. Imaging in high resolution was performed after the sample was cooled down to room temperature, at sample biases between -2 V and $+2$ V and a tunnel current of 0.2 nA. We observed the diffusion of Ti adsorption structures *in situ* at temperatures between 557 K and 630 K. Before evaporating Ti, we waited 1–2 h until the drift rate of a STM image reduced to < 0.01 Å/sec. Low Ti coverage of 0.002–0.01 ML was used to avoid possible interactions and misidentification of Ti adsorption structures. We used sample biases of -1.2 V and $+0.8$ V, and tunneling current of 0.1 nA. The area of 200×200 Å² was scanned successively at 5.5 sec intervals for 10 min–1 h. The successive images of the hopping motion are recorded by videocassette recorder and analyzed later on. The system pressure was kept about $1\text{--}2\times 10^{-10}$ Torr during the Ti evaporation and the high-temperature observations.

III. RESULTS

A. Adsorption structures and reaction

Figure 1 shows images of a Si(001)- 2×1 surface on which Ti is evaporated up to $\Theta_{\text{Ti}} = 0.01$ ML. Most of the deposited Ti is seen as bright protrusions on the 2×1

dimer rows. The arrowed features are Ti atoms adsorbed nearly at valley bridge sites, though such different adsorption sites are less than approximately 5% of the total adsorption structures. By comparing the number density of the adsorption structures with the deposition amount, the adsorption structure is identified to be a monatomic structure. Preferred adsorption at step edges is scarcely seen.

Figure 2 shows Ti adsorption structures on dimer rows, which is a dominant adsorption site. Ti adsorption structures at different biases are seen in common as protrusions centered between two neighboring dimer pairs, i.e., at the pedestal sites. The peak height of the protrusions relative to the top of the dimer row is measured to be ~ 0.4 Å at -1.1 V and ~ 1 Å at $+0.8$ V as indicated in Fig. 2(c).

As shown in Fig. 3, taken at 460 K, we have observed conversion of Ti adsorption structures from the bright protrusions to dark patches on dimer rows. This conversion is observed as a sudden change of image contrast between the successive images taken at ~ 18 sec intervals. It was observed at temperatures higher than 440 K during the course of the observation up to ~ 1 h. Significant mobility is not seen before the conversion at this temperature. Displacement of the structures before and after the conversion was measured to be 1.9 Å, which corresponds to half of a dimer-dimer spacing.

We show high resolution images of the high-temperature adsorption structures of Ti formed by depositing at 700 K and quenched at RT in Fig. 4. At a negative sample bias of -1.0 V, a Ti adsorption structure is seen as a recessed dimer similar to a single dimer vacancy (SDV) in the same image. In the profiles along dimer rows, the recession at the Ti site is smaller than that for the pure dimer vacancy by ~ 0.3 Å at -1.0 V and ~ 0.8 Å at $+1.0$ V. Another distinct feature is the rise of the several dimers neighboring the central recession of ~ 0.5 Å at -1.0 V. Also at $+1.0$ V, they are distinctive from the separated dimer atoms near the dimer vacancy. In the experimental bias range from -2 V to $+2$ V, the structure is essentially symmetric about the axes along and perpendicular to the dimer row.

Figure 5 shows the morphologies induced by Ti deposition at 558 K at lower magnification. At this sample

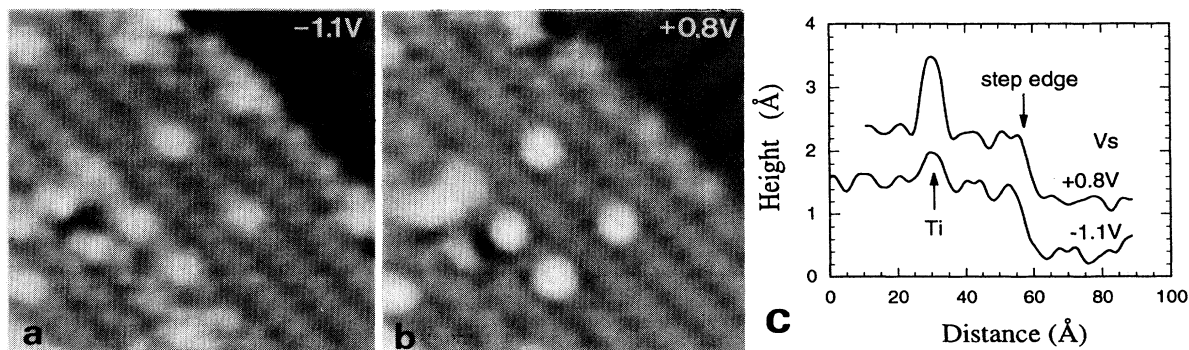


FIG. 2. Adsorption structure of Ti at pedestal sites at RT taken at sample biases of (a) -1.1 V, (b) $+0.8$ V, and (c) corresponding image profiles.

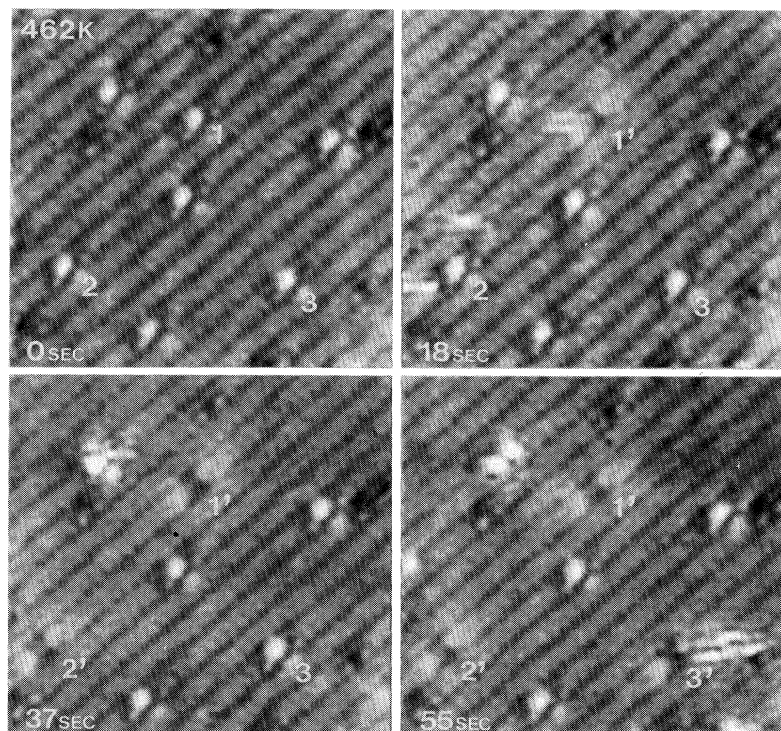


FIG. 3. Conversion from the low-temperature adsorption structures (1–3) to the high-temperature adsorption structures (1'–3'). Images are taken successively at ~ 18 sec intervals at 462 K. Sample bias and tunnel current are +1 V and 0.15 nA, respectively.

bias of -1.9 V, the Ti sites show a dark feature similar to the dimer vacancies. From the measurement at positive biases, at which Ti sites show distinctive contrast, we have found no increase of the number of vacancies with Ti coverage but an increase of the number of Ti sites with Ti coverage. At $\Theta_{\text{Ti}} = 0.2$ ML, the initial growth of three-dimensional (3D) clusters becomes significant.

Particularly to be noticed here is the formation of 1D strings and 2D islands seen brightly on the terrace. The anisotropic island shapes and the coarsening of step edges seen in Fig. 5(b) are similar to that seen for Si homoepitaxy.¹² They are identified as Si dimer islands also by the bias dependence as shown in Fig. 6, which

is common to that of the substrate 2×1 terrace. In the experimental temperature range, formation of 2D surface structure induced by the Ti adsorption is not found, other than the Si dimer islands.

We estimated the number of Si atoms in the dimer islands N_{Si} by measuring the coverage of the dimer islands. Measurements were carried out for the area in the middle of terraces as wide as several hundred to one thousand angstroms for minimizing the influence of step edges. The result is shown in Fig. 7 as a function of the number of Ti adsorption structures N_{Ti} measured at positive sample biases. The number of the adsorption structures increases corresponding to the deposited Ti amount

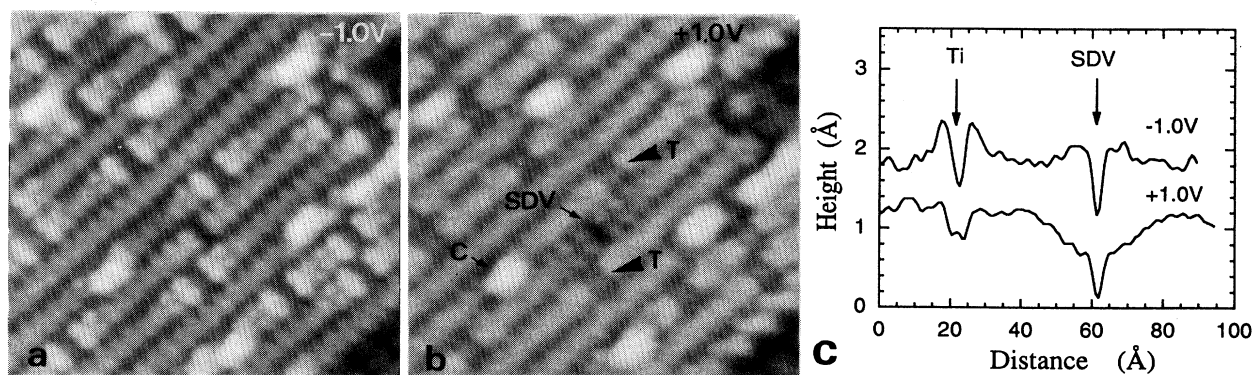


FIG. 4. Sample bias dependent topographies of Ti adsorption structures (T) formed by deposition at 700 K and quenching to RT taken at (a) -1.0 V, and (b) $+1.0$ V. (c) Image profiles along a dimer row. “SDV” denotes an intrinsic single dimer vacancy, and “C” a “C type” dimer defect (Ref. 18).

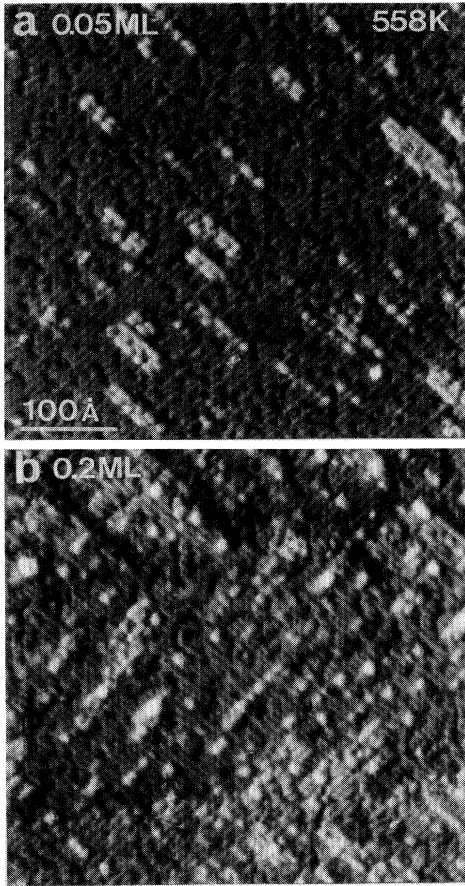


FIG. 5. Wide views taken at 558 K at $\Theta_{\text{Ti}} =$ (a) 0.05 ML; (b) 0.2 ML. Sample bias is -1.9 V.

$\Theta_{\text{Ti}} < 0.1$ ML and tends to saturate for $\Theta_{\text{Ti}} \geq 0.1$ ML. The saturation occurs for the coverage region in which the growth of 3D clusters becomes significant. However, the ratio $N_{\text{Si}}/N_{\text{Ti}}$ is approximately 2 over the measurement coverage up to 0.2 ML.

B. Diffusion of adsorption structure

In Fig. 8, we present typical snapshots of the hopping motion of the adsorption structures taken successively at 12 sec intervals. We focus our attention on isolated Ti adsorption structures to characterize the hopping motion. We have observed a total of about 4000 displacement events and have found that the diffusion motion is strictly restricted along the dimer row. We have not detected a motion perpendicular to the dimer row. The adsorption structures displace discretely, i.e., “hop” between the neighboring adsorption sites by a unit length of 3.8 \AA . With these observations, we assume that the hopping motion is modeled as a one-dimensional (1D) random walk. The hop rate ν_H relates to the 1D displacement of a Ti adsorption structure Δx in time Δt as

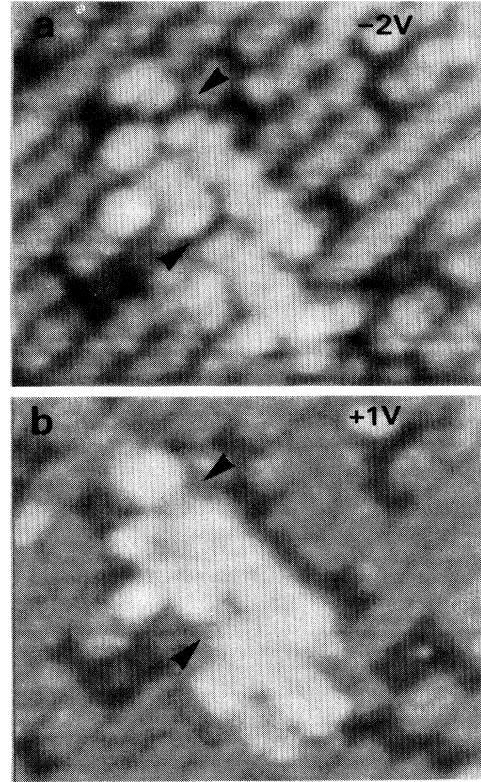


FIG. 6. A small dimer island at biases of (a) -2 V and (b) $+1$ V. Arrows indicate Ti adsorption structures formed on the island.

$$\langle \Delta x^2 \rangle = \nu_H \Delta t, \quad (1)$$

$$\nu_H = \nu_{H0} \exp(-E_D/kT), \quad (2)$$

where E_D is the activation energy for diffusion and ν_{H0} is the prefactor for the hop rate.¹³ Measurements were carried out for the isolated adsorption structures while they do not closely encounter the others as seen in Fig. 8(d). For a particular temperature, the displacements of 10–30 Ti adsorption structures were read at time intervals of Δt . The number of displacement events for a single adsorption structure during the observation duration is typically 10–20 for 30 min at 558 K and 20–40 for 5 min at 630 K. We have confirmed the linear relationship of Eq. (1) by varying Δt from 5.5 sec to 200 sec. We have also measured hop rates at $\Delta t = 15$ min during which the probe tip has shifted away about 1000 \AA from the measurement area. This procedure should reduce the possible interaction between the tip and the Ti adsorption structures by a factor of 10^2 compared to that for the successive scan at 5.5 sec intervals. As a result, the hop rates measured by the two methods were consistent within the measurement uncertainty. This indicates small tip-induced effects in the present observation.

The measured hop rate ν_H is shown as a function of temperature in Fig. 9. We obtain the activation energy for diffusion of $E_D = 1.8 \pm 0.1$ eV and the prefactor of $\nu_{H0} = 10^{14 \pm 1} \text{ sec}^{-1}$.

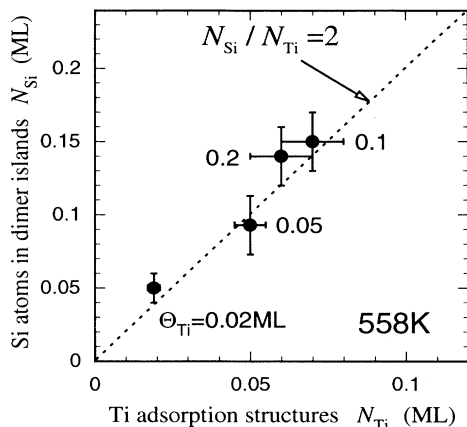


FIG. 7. Number of Si atoms in dimer islands (N_{Si}) as a function of the number of Ti adsorption structures (N_{Ti}) at 558 K. Evaporated Ti coverage (Θ_{Ti}) is indicated for each plot.

IV. DISCUSSION

From the STM images of the low-temperature (LT) adsorption structure, it is attributed that a Ti atom adsorbs at the pedestal site as schematically shown in Fig. 10(a). Besides, the measurement of the coverage of Si dimer islands at elevated temperature is an indication that the formation of one high-temperature adsorption structure forms two Si atoms on the terrace. This and the recessed image contrast are consistently explained by modeling the high-temperature (HT) adsorption structure as

shown in Fig. 10(a). This is schematically described as “a single dimer vacancy on which a Ti atom adsorbs.” Taking the symmetric image feature into account, the adsorption site of a Ti atom is considered to be at the center of the dimer vacancy. Because of the image profiles changing with sample bias, estimation of the height of a Ti atom could be valid by assuming that the Ti-Si distances are within the range of those in known silicides C49-TiSi₂ and C54-TiSi₂ of 2.54–2.86 Å (Ref. 14) and no significant displacement of the surrounding atomic configuration. For the high-temperature adsorption site, the vertical position of Ti is estimated to be nearly the height of the second Si layers. The low-temperature site of a Ti atom is estimated to be 1.1–1.8 Å above the dimer level. However, considering the profile measurement, the height of a Ti atom is thought not to be considerably higher than ~1 Å.

As shown in Fig. 10(b), the conversion process of the two adsorption structures is described below. The displacement with the site conversion indicates that it occurs between the adjacent adsorption sites and that the ejection of one of the two dimer pairs neighboring the adsorbed Ti at the pedestal site is activated on the site conversion path. The ejected Si atoms migrate on the terrace and nucleate to form Si dimer islands. The absence of the ejected Si monomers in the images is explained by the high mobility of the Si monomer of 10^3 – 10^4 hops sec^{-1} at the experimental temperature.⁷ Additionally, the decrease of N_{Ti} and N_{Si} seen for $\Theta_{\text{Ti}} \geq 0.1$ ML can be attributed to the capture of incident Ti by the growing 3D clusters.

The measured diffusivity and the activation energy are close to those for the bulk diffusion of Ti in Si with

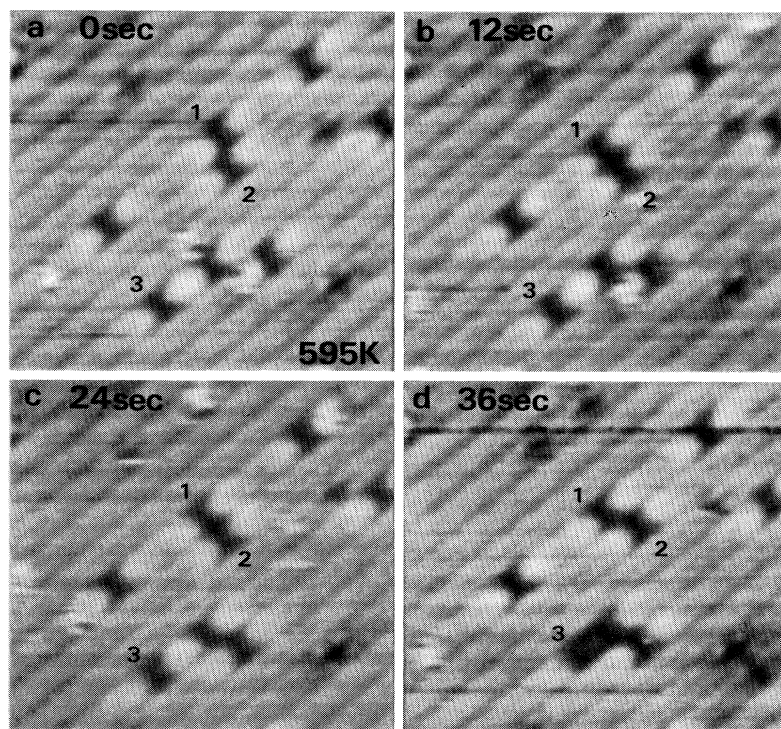


FIG. 8. Four successive images taken at intervals of 12 sec at 595 K. Ti adsorption structures “hop” along dimer rows. Three of the adsorption structures are numbered for easy identification.

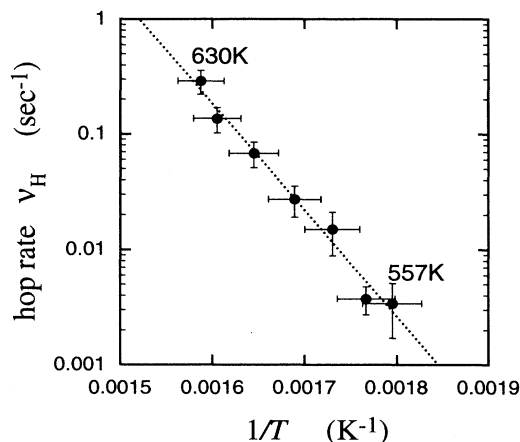


FIG. 9. Arrhenius plot for the measured hop rate ν_H of Ti adsorption structures. The activation energy for diffusion and the prefactor are measured to be $E_D = 1.8 \pm 0.1$ eV and $\nu_{H0} = 10^{14 \pm 1}$ sec⁻¹, respectively. Horizontal error bars refer to ± 10 K.

$E_D = 1.79$ eV.¹⁵ However, it seems that the interstitial diffusion suggested for the bulk diffusion cannot be applied simply to our structural model. Instead, we propose another possible mechanism consistent with the modeled adsorption structure. Apparently from the structural feature of our model, its hopping process should

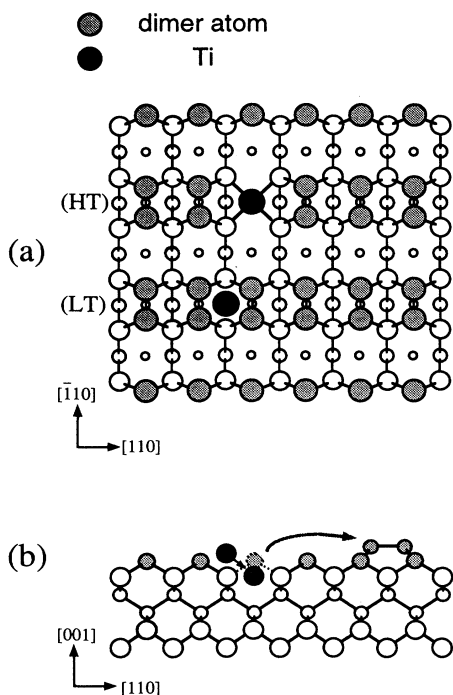


FIG. 10. (a) Models for adsorption structures at low temperature (LT) and elevated temperature (HT). (b) Site conversion process of Ti at elevated temperature involving the adsorption at the pedestal site, conversion to the site at the second layer, and ejection of Si dimer atoms.

include a displacement of a Ti atom and the surrounding dimer vacancy structure. For the diffusion of the intrinsic SDV on Si(001)- 2×1 , a STM measurement by Kitamura *et al.*¹⁰ and a calculation by Zhang *et al.*¹⁶ have given $E_D = 1.7 \pm 0.4$ eV and $E_D = 1.4 - 1.6$ eV, respectively. The displacement mechanism was modeled as “a coherent exchange of pairs of Si atoms between the top and the second layer.” This model excludes the breakage of strong Si-Si bonds which would require an activation energy considerably higher than 2 eV. The comparable activation energy with that for the SDV indicates that a displacement mechanism of the Ti adsorption structure possibly involves a similar site exchange process without bond breakage.

The dimer ejection indicates that the high-temperature site is energetically more favorable than the low-temperature site and that the dimer ejection is activated by the energy gain due to the site conversion. The higher stability of the higher-temperature adsorption is also estimated by the duration of the adsorption structure much longer than that for SDV at least by three orders of magnitude.¹⁰

A comparison with the intrinsic SDV provides information about the stability of the high-temperature adsorption structure. In the case of SDV, at the second layer atoms displace about 0.5 Å toward the center of the vacancy and rebond to terminate the dangling bonds.¹⁷ This also induces tensile strain on the adjacent atoms. In the high-temperature adsorption structure, the second layer Si atoms are fully coordinated. On the assumption that the Ti is exactly at the second layer, horizontal displacement of the second layer atoms is estimated to be -0.2 Å through $+0.3$ Å. Thus, in this structure, the four dangling bonds can be terminated without introducing such a large strain as the SDV does. Therefore the high-temperature adsorption structure is considered to be more energetically favorable than the SDV. Experimentally, the structural modulation as discussed above is indicated by the change in image contrast on the dimers neighboring the central Ti site. For the low-temperature site, the underlying Si dimer atoms are undercoordinated differently from the high-temperature adsorption site. This is consistent with the estimated higher total energy of the structure. Moreover, with the modeled reaction path, it is considered that the formation energy of the dimer vacancy of 0.22 eV (Ref. 17) gives the lower limit of the energy difference between the two adsorption structures.

Also the significant reduction of the hop rate can be explained by the stability of the high-temperature adsorption structure. The alternate contribution of the increasing activation energy and the decreasing prefactor could not be separated because of the error ranges of the hop rate measurements to be compared. Therefore we cannot estimate to which, the activation energy or the prefactor, the strong Ti-Si bonds and the release of the strain contribute. However, we can possibly understand that the lowering of the energy at the equilibrium state can cause the higher barrier height for the atomic displacement. Moreover, the estimated strong Ti-Si bonding configuration supports the diffusion mechanism with

a rebonding process rather than a bond breaking process.

For a more detailed discussion on the energetics, a theoretical investigation has to be carried out.

V. SUMMARY

We have observed two adsorption structures characteristic for temperatures below and above 440 K, at the monatomic adsorption stage of Ti on Si(001), and the reaction path is modeled with the *in situ* observation of the site conversion. The growth features of both adsorption structures have been attributed to the preference of Ti-Si bond formation, which is reflected significantly on the ejection of dimer Si atoms. Moreover, the stability of the Ti-Si bonding configuration is also indicated by the comparison of the diffusivity between the Ti adsorption structure and the intrinsic dimer vacancy. However, their diffusion mechanisms are commonly explained by the coherent exchange mechanism of atoms because their acti-

vation energies are lower than that required for a bond breaking process.

We believe the present observations provide information on elemental processes at the growing reactive Ti/Si interface and show a precursor of silicidation. In the formation of the interfacial mixing layer by RT deposition and an annealing procedure, a similar type of bond weakening/breakage reaction with a site exchange process possibly takes place and is an elemental process of the interfacial mixing. Moreover, the bulk diffusivity of Ti in Si much smaller than that for the other 3d metals¹⁵ might be affected by the strong Ti-Si bonding configuration, as is suggested for the surface diffusion in this paper.

ACKNOWLEDGEMENT

We thank our colleague K. Miwa at Toyota R&D Laboratories for insightful discussions on adsorption reaction.

* To whom all correspondence should be addressed. Also at Department of Applied Physics, Nagoya University, Nagoya 464-01, Japan. Electronic address: e0779@mosk.tytlabs.co.jp

¹ M. Iwami, S. Hashimoto, and A. Hiraki, *Solid State Commun.* **49**, 459 (1984).

² M.D. Giudice, J.J. Joyce, M.W. Ruckmann, and J.H. Weaver, *Phys. Rev. B* **35**, 6213 (1987).

³ X. Wallart, J.P. Nys, H.S. Zeng, G. Dalmai, I. Lefebvre, and M. Lannoo, *Phys. Rev. B* **41**, 3087 (1990).

⁴ M. Azizan, T.A. Nguyen Tan, R. Cinti, R. Baptist, and G. Chauvet, *Surf. Sci.* **178**, 17 (1986).

⁵ J.G. Clabes, G.W. Rubloff, and T.Y. Tan, *Phys. Rev. B* **29**, 1540 (1984).

⁶ T.A. Nguyen Tan, M. Azizan, and J.Y. Veuillen, *Surf. Sci.* **251/252**, 428 (1991).

⁷ Y.W. Mo, J. Kleiner, M.B. Webb, and M.G. Lagally, *Phys. Rev. Lett.* **66**, 1998 (1991).

⁸ Y.W. Mo and M.G. Lagally, *Surf. Sci.* **248**, 313 (1991).

⁹ E. Ganz, S.K. Theiss, I.S. Hwang, and J. Golvochenko, *Phys. Rev. Lett.* **68**, 1567 (1992).

¹⁰ N. Kitamura, M.G. Lagally, and M.B. Webb, *Phys. Rev. Lett.* **71**, 2082 (1993).

¹¹ Y.W. Mo, *Phys. Rev. Lett.* **71**, 2923 (1993).

¹² M.G. Lagally, *Kinetics of Ordering and Growth at Surfaces* (Plenum Press, New York, 1990).

¹³ R. Gomer, *Rep. Prog. Phys.* **53**, 917 (1990).

¹⁴ W.B. Pearson, *Crystal Chemistry and Physics of Metals and Alloys* (Wiley, New York, 1972).

¹⁵ S. Hocine and D. Mathiot, *Appl. Phys. Lett.* **53**, 1269 (1988).

¹⁶ Z. Zhang, H. Chen, B.C. Bolding, and M.G. Lagally, *Phys. Rev. Lett.* **71**, 3677 (1988).

¹⁷ J. Wang, T.A. Arias, and J.D. Joannopoulos, *Phys. Rev. B* **47**, 10 497 (1993).

¹⁸ R.J. Hamers and U.K. Köhler, *J. Vac. Sci. Technol. A* **7**, 2854 (1989).

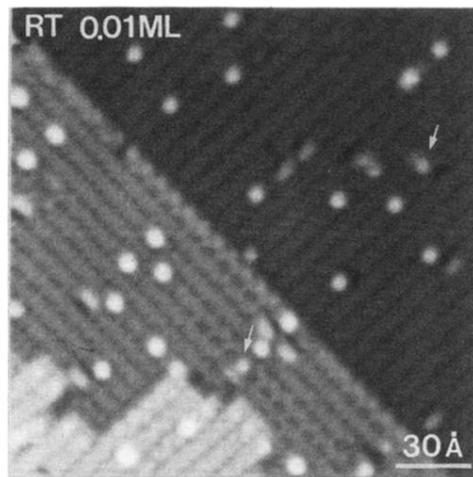


FIG. 1. Morphologies of Si(001)- 2×1 surface with Ti deposited up to $\Theta_{\text{Ti}} = 0.01$ ML. The image is taken at a sample bias of +2 V. Arrows indicate adsorption at valley sites.

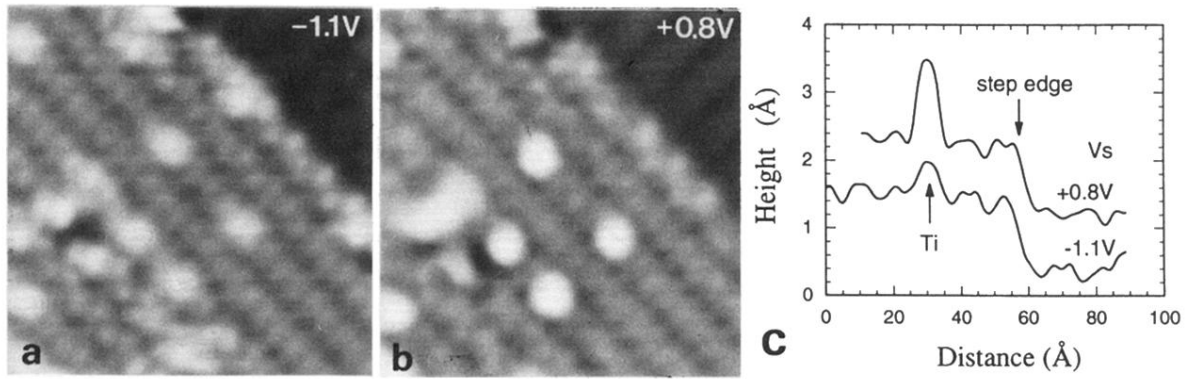


FIG. 2. Adsorption structure of Ti at pedestal sites at RT taken at sample biases of (a) -1.1 V, (b) $+0.8$ V, and (c) corresponding image profiles.

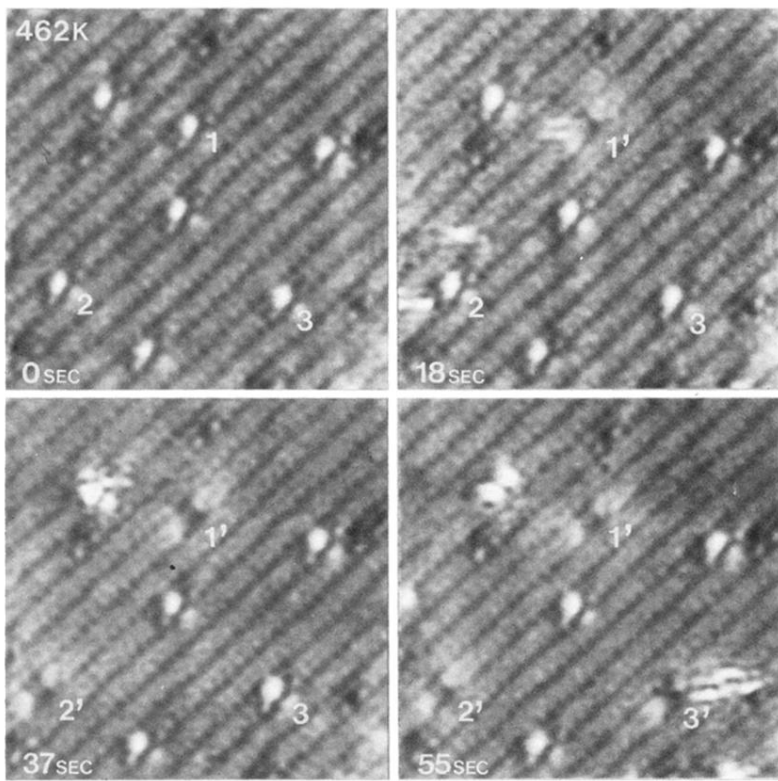


FIG. 3. Conversion from the low-temperature adsorption structures (1-3) to the high-temperature adsorption structures (1'-3'). Images are taken successively at ~ 18 sec intervals at 462 K. Sample bias and tunnel current are +1 V and 0.15 nA, respectively.

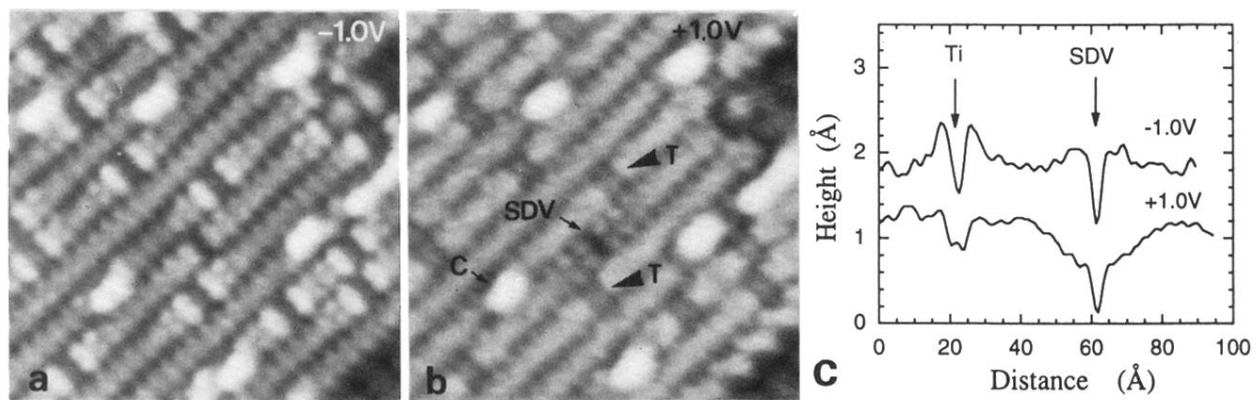


FIG. 4. Sample bias dependent topographies of Ti adsorption structures (T) formed by deposition at 700 K and quenching to RT taken at (a) -1.0 V, and (b) $+1.0$ V. (c) Image profiles along a dimer row. “SDV” denotes an intrinsic single dimer vacancy, and “C” a “C type” dimer defect (Ref. 18).

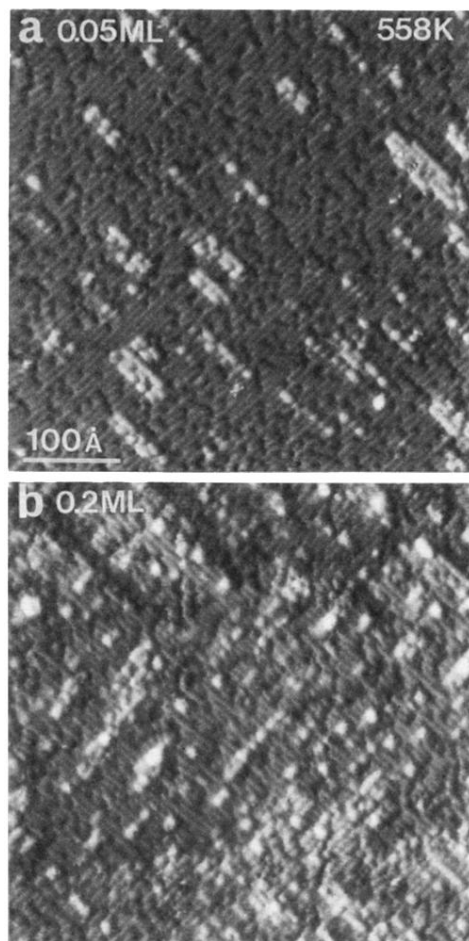


FIG. 5. Wide views taken at 558 K at $\Theta_{T_i} =$ (a) 0.05 ML; (b) 0.2 ML. Sample bias is -1.9 V.

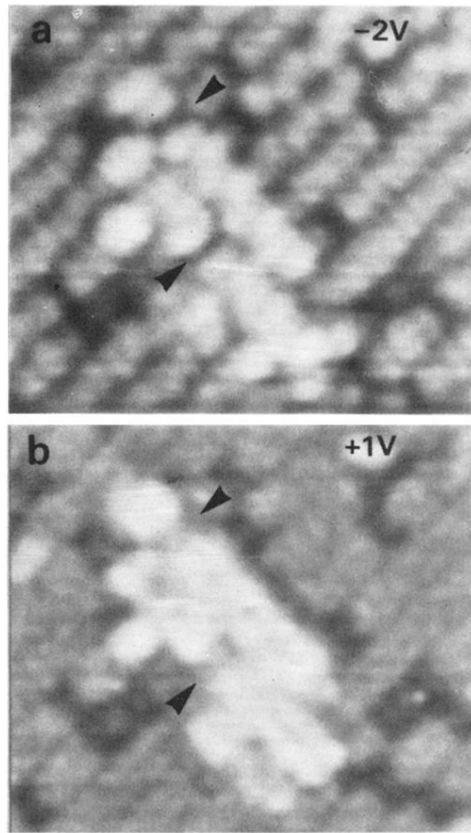


FIG. 6. A small dimer island at biases of (a) -2 V and (b) $+1$ V. Arrows indicate Ti adsorption structures formed on the island.

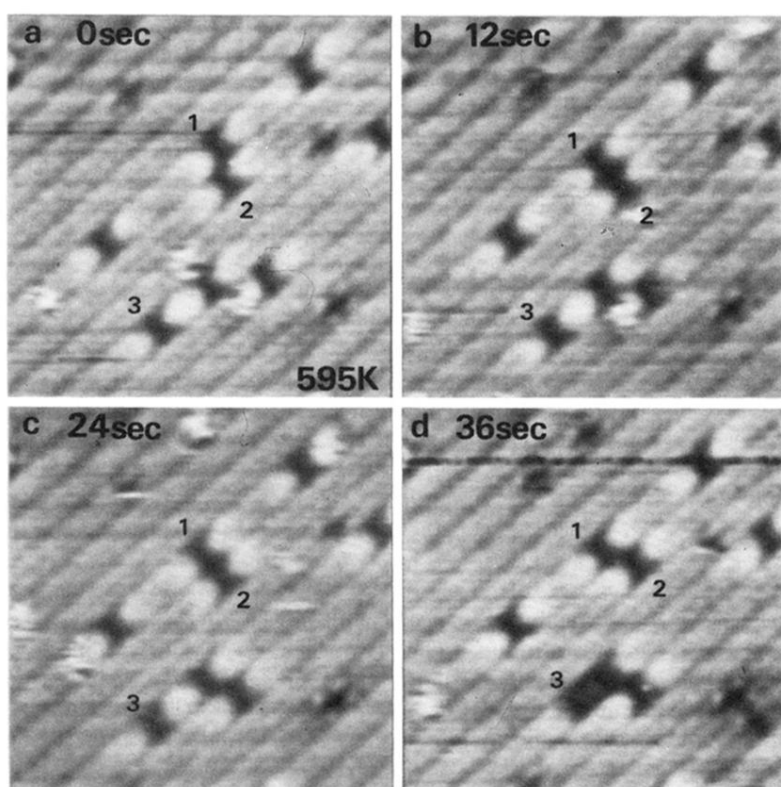


FIG. 8. Four successive images taken at intervals of 12 sec at 595 K. Ti adsorption structures “hop” along dimer rows. Three of the adsorption structures are numbered for easy identification.